

The Tevatron Tripler: How to Upgrade the Fermilab Tevatron for the Higgs Boson and Supersymmetry

P. McIntyre, E. Accomando, R. Arnowitt, B. Dutta, T. Kamon, and A. Sattarov

Department of Physics, Texas A & M University, College Station, TX 77843

(August, 1999)

Recent advances in superconductor properties and superconducting magnet technology have made it possible to build cost-effective, high-performance dipoles with a field of 12 Tesla - 3 times the field strength of the Tevatron. Such magnets could be used to upgrade Fermilab's collider in its existing tunnel to a collision energy $\sqrt{s} = 6$ TeV and luminosity $\mathcal{L} > 10^{33} \text{ cm}^{-2}\text{s}^{-1}$. We have calculated the parton luminosities for quark-antiquark and gluon-gluon scattering for the Tevatron, the Tripler, and LHC. In most models of the Higgs field and supersymmetry, the Tripler would have a high likelihood to discover many of the predicted particle states.

PACS numbers: 14.80.Bn, 14.80.Ly, 07.55.Db, 29.20.-c

Accelerator technology has paced the discovery of new particles at hadron colliders. With the invention of beam cooling techniques [1,2], it became possible to make colliding beams of protons and antiprotons in existing accelerators [3]. $p\bar{p}$ colliding beams make use of the valence antiquarks within the antiproton to access the annihilation channels through which many new particles are produced most directly. This development led to the discovery of the weak bosons [4]. With the development of superconducting accelerator magnets [5], it became possible to extend the energy reach in collisions to 2 TeV, leading to the discovery of the top quark [6]. Continuing progress towards higher collision energy for hadron collisions requires the development of magnets with yet higher magnetic field strength. Three properties of high-field dipoles have so far inhibited such progress: the intrinsic performance of the superconductor, degradation of the superconductor by mechanical stress, and protection of the magnet in the event of quench.

I. OPTIMIZATION OF HIGH-FIELD DIPOLES

The alloy NbTi has been used as the superconductor for all superconducting colliders: Tevatron, HERA, RHIC, and now LHC [7]. This alloy makes a very robust cable and has been perfected to a high-performance technology. Unfortunately its upper critical field limits the maximum field that can be produced, so that even cooling with superfluid helium (1.8^0K) the 8.4 Tesla field of the LHC is a practical limit (Figure 1).

Nb₃Sn has recently matured as a practical superconductor, so that strand is now available with a current density $j_{sc} = 2,000 \text{ A/mm}^2$ at 12 Tesla [8]. Bi-2212 strand is now reaching $1,000 \text{ A/mm}^2$, with an upper critical field above any practical field strength. While these new conductors in principle offer much higher field strength for dipoles, they are brittle materials and

undergo strain degradation of supercurrent capacity j_c at moderate stress levels. Figure 2 shows the dependence of j_c on stress in the superconducting filaments of multi-filament Nb₃Sn strands made by three processes - powder-in-tube (PIT), bronze, and modified jelly roll (MJR). Only the MJR process yields high $j_c(0)$, but it exhibits the largest degradation from strain, so that coil stress must be limited to $\sim 120 \text{ MPa}$. Bi-2212 is even more brittle, degrading at stresses of $\sim 70 \text{ MPa}$. The stress from the Lorentz forces in a dipole coil accumulates from the inside to the outside of the coil. For a central field of 12 Tesla, the peak stress in a conventional multi-shell $\cos\theta$ coil would reach $\sim 150 \text{ MPa}$.

A technique of stress management was devised recently, in which a support matrix is integrated within the coil [9]. The matrix of high-strength ribs and plates intercepts the stresses acting on the inner coil elements and bypasses them past the outer elements, so that stress cannot accumulate beyond $\sim 70 \text{ MPa}$. Since the matrix material (e.g. Inconel) can support much greater loading stress than the fragile coils, this approach effectively removes mechanical stress as a limit for high-field magnet technology.

A remaining limit to high-field dipole technology is the requirement that the coil not be damaged in the event that it loses its superconducting state (quench). The coil consists of an array of windings, each a rectangular (Rutherford) cable containing ~ 30 -40 superconducting strands. Each strand in turn contains ~ 300 -1000 filaments of superconductor drawn within a copper matrix. The main cost in making superconducting strand is the complex sequence of stacking, extruding, drawing, and heat treatment needed to achieve optimal superconducting performance. Since the cost scales with the volume of processed strand, *the added copper costs as much as the superconductor itself*.

Figure 1 shows the critical current vs. field in the filaments of several practical superconductors. The mag-

netic field in the superconducting coil is largest in its inner regions, and decreases and even reverses direction in its outer regions. In an optimized series coil, the inner windings would have smaller cross-section, and the outer windings would have larger cross-section. This optimization is called grading, and optimally uses the available current density $j_c(B)$ throughout the coil.

When a coil quenches, however, the current still must be carried in the quenched regions of each winding. Since superconducting alloys are quite resistive in the normal state, a substantial amount of a good conductor (e.g. copper) must be integrated into the cables. Copper is required for two reasons. A modest amount of copper is needed to *stabilize* the superconducting filaments so that when a single filament quenches, the surrounding copper can carry the current and conduct heat from the quenched filament sufficiently that the filament can regain its superconducting state. Quench stability for high field Nb_3Sn coils typically requires an amount of copper equal to about 40% of the strand cross-section.

Copper is also required to *protect* the coil in the event that an entire region of cable begins to quench. During such quench the current must be transferred to the copper so that heat dissipation can be limited sufficiently that the stored magnetic field energy can be safely dissipated throughout the cold mass of the magnet. This condition requires that sufficient copper be distributed in the cable so that the current density in copper during quench is $j_{Cu} < 1,500$ A/mm².

Conventionally all of the copper for both stability and quench protection is extruded as a matrix within each multi-filament strand. We recently devised an alternative strategy [10], in which only the copper for quench stability is integrated within the strand, but the (typically much larger amount of) copper for quench protection is provided by cabling pure copper strands together with copper-stabilized superconducting strands in each cable. The proportion of copper and superconducting strands is chosen to provide the necessary quench protection in each region of the coil.

Figure 3 shows the design of a 12 Tesla dipole that contains provisions for stress management and also an optimized arrangement of copper and superconductor in the cables. The inner segment of the coil uses cable containing two superconducting strands for each copper strand. The middle segment of the coil uses cable containing equal numbers of copper and superconducting strands. The magnetic field in the outer segment is everywhere less than 7.2 Tesla, and so high-performance $NbTi$ cable can be used there (half of the entire coil).

The impact of this design approach can be appreciated by comparing the coil area required for conventional dipoles and for designs using the above innovations. Figure 4 shows the coil cross-section area for each of the $NbTi \cos\theta$ dipoles of existing colliders, and for three designs using the above design strategy: the 12 Tesla Tripler dipole of Figure 3 (only the Nb_3Sn coil area is counted for this purpose), a 15 Tesla all- Nb_3Sn

dipole, and finally a 20 Tesla dipole using Bi-2212 inner coils and Nb_3Sn outer coils. These last two designs have reduced aperture (4 cm) and may be appropriate for a future ultimate-energy hadron collider (VLHC). The amount of superconductor required for conventional designs increases quadratically with field, while the superconductor required for the optimized designs increases linearly. The high-field designs require far less superconductor/TeV than do dipoles for the SSC and LHC.

II. TEVATRON TRIPLER

The new dipole design strategy makes it possible to upgrade Fermilab's Tevatron by replacing its ring of 4 Tesla dipoles by a ring of 12 Tesla dipoles. In addition to the high-field dipoles, the upgraded ring requires quadrupoles with 3 times the gradient of those used in the Tevatron. A block-coil Nb_3Sn quadrupole with the necessary gradient has been designed.

The new magnets could be installed on the existing stands that until recently supported the original Main Ring. The Tripler would make colliding beams with a collision energy $\sqrt{s} = 6$ TeV. The antiproton source, injectors, cryogenics, RF systems and detectors of the Tevatron could all be used with modest upgrade.

The luminosity of the Tripler is

$$L = \frac{N_b N_p N_{\bar{p}} f}{\beta^* \sqrt{\epsilon_h \epsilon_v}} \gamma = 10^{33} \text{ cm}^{-2} \text{ s}^{-1} \quad (1)$$

where $N_b = 160$ is the number of bunches, $N_p = 3 \times 10^{11}$ and $N_{\bar{p}} = 4 \times 10^{10}$ are the numbers of particles per bunch, $f = 50$ kHz is the revolution frequency, $\beta^* = 0.25$ m is the focal length at the collision point, and ϵ_h and ϵ_v are the invariant emittances in the horizontal and vertical phase space of the beam. The luminosity scales with the relativistic γ of the beam. All of the other parameters are the same for the Tripler as they will be for the Tevatron as that being upgraded for its next run.

The Tripler must accommodate counter-circulating beams of protons and antiprotons. For high-luminosity collisions, the beams must be fully separated everywhere except at the two locations where they collide inside the detectors, so that beam-beam tune shift is minimized. This is accomplished using electrostatic deflectors, so that the two beams trace a double helix within the beam tube of the dipoles. The 6 cm aperture of the design in Figure 3 is sufficient for this purpose.

A last requirement is that the field distribution in the dipoles be sufficiently uniform so that high luminosity can be maintained during a days-long store. This requirement is usually expressed by requiring that the multipoles b_n should be smaller than $\sim 10^{-4} \text{ cm}^{-n}$. We achieve this criterion by current-programming the inner windings. Figure 5 shows the multipoles vs. field over the 20:1 range from injection to collision energy. At 12 Tesla, synchrotron radiation is not yet enough to require

the use of an intermediate-temperature liner in the beam tube. The total radiated power in the ring is

$$P = \frac{2e^6 c^2}{9\epsilon_0 (m_p c^2)^4} E^2 B^2 N_b (N_p + N_{\bar{p}}) = 400W \quad (2)$$

This power could be removed using the installed cryogenic refrigeration capacity in the Tevatron.

III. PARTON LUMINOSITIES

In order to assess the potential of the Tripler for the discovery of new particles, we have calculated parton luminosities with which the constituents of colliding hadrons interact. Parton luminosities are calculated for $u\bar{d}$ scattering and for gluon-gluon scattering, for the cases of the Tevatron, the Tripler, and the LHC. The calculations use the CTEQ4 parton distributions [11]. The results are presented in Figure 6 as a function of $\sqrt{\hat{s}}$, the c.m. energy for the colliding partons. The signals for the Higgs boson and for supersymmetry (SUSY) at a hadron collider sort into two broad categories: those with signatures of multiple leptons and missing energy, for which the cross-sections are small but the signal/background ratio is fairly large; and those with signatures of multiple quarks (jets) and missing energy, for which the cross sections are larger but the signal/background ratio is small. The multi-lepton states are accessed primarily through quark-antiquark annihilation, while the multi-quark states are accessed primarily through gluon fusion. Searches for Higgs and SUSY states at the Tevatron concentrate primarily on the multi-lepton signatures, taking advantage of the valence antiquark content of the antiproton that enhances the high-mass spectrum of quark-antiquark annihilation (Figure 6). The preparation for similar searches at LHC concentrates on the multi-quark signatures, since for pp collisions an antiquark must be drawn from the sea with reduced \hat{s} .

To evaluate the signals and backgrounds for the several signatures for Higgs and SUSY as a function of mass scale, one must conduct a detailed Monte Carlo generation of events and simulation of detector cuts and acceptances. This work is in progress. A first estimate of sensitivity can be obtained by extrapolating the fully simulated signals and backgrounds for each signature that have been done by the CDF and D0 collaborations in preparation for Run II of the Tevatron [12]. The yields of signal events are scaled from the Tevatron simulation, using the integrated luminosities for scattering from Figure 6 for parton c.m. energies greater than $M_H + M_Z$. Similarly the background events are scaled from the Tevatron simulation using the gluon-gluon luminosities. Table 1 presents the signals and background for a 20 fb^{-1} data sample (a one-year run at the Tripler luminosity). Also presented are the χ^2 that would result from a Bayesian combination of the several signatures. The 95% confidence limit would extend to $400 \text{ GeV}/c^2$ mass scales.

In previous studies, SUSY [13] and Higgs [14] signals were evaluated for a proposed 4 TeV upgrade of the Tevatron. Extrapolating from those results, the Tripler should be sensitive to gluinos and squarks with masses up to $\sim 750 \text{ GeV}$, and would be able to see the trilepton signal (associated production of chargino and neutralino) over much of the interesting parameter space for both universal and non-universal soft breaking.

IV. CONCLUSION

The new developments in superconducting dipole design make it feasible to extend the high-field frontier for future hadron colliders. The Tripler is a first opportunity to use this technology to advantage, extending the reach for Higgs and SUSY particles to $>500 \text{ GeV}/c^2$. Its extension of the reach for quark annihilation processes is complementary to the primarily gluon-mediated processes at LHC, and the lepton annihilation channels at NLC. For this reason the Tripler would remain a competitive facility through much of the physics life of LHC and NLC.

It is a pleasure to acknowledge stimulating discussions with W. Barletta and R. Scanlan of LBNL, and R. Noble of Fermilab. This work was supported by DOE grant DE-FG03-95ER40924, NSF grant PHY-9722090, and by a Texas Advanced Technology Program grant.

-
- [1] G. Budker and A. Skrinsky, Usp. Fiz. Nauk. 124, 561 (1978).
 - [2] S. Van der Meer et al., Physics Reports 58, 73 (1980).
 - [3] D. Cline, P. McIntyre, and C. Rubbia, "How to observe the weak bosons in proton-antiproton collisions using existing accelerators", Proc. Int. Neutrino Conf., Aachen, 683 (1976).
 - [4] G. Arnison, et al., Phys. Lett. B122, 103 (1983).
 - [5] R.R. Wilson, The Tevatron, Physics Today 10, 23 (1977).
 - [6] F. Abe et al., Phys. Rev. Lett. 74, 2626 (1995); S. Abachi et al., Phys. Rev. Lett. 74, 2632 (1995).
 - [7] L. Evans, "LHC accelerator physics issues and technology challenges", Proc. Particle Accel. Conf., New York, March 29, 1999.
 - [8] T. Pyon and E. Gregory, "Niobium-Tin for fusion, high energy physics and other applications", Proc. Conf. on Applied Superconductivity, Palm Desert, CA, Sept. 25-30, 1999.
 - [9] T. Elliott et al., "Stress management in high-field dipoles", Proc. Particle Accel. Conf, Vancouver, May 12-16, 1997.
 - [10] C. Battle et al., "Optimization of block-coil dipoles for hadron colliders", Proc. Particle Accelerator Conf., New York, NY, March 30-April 1, 1999.
 - [11] H. Lai et al., Phys. Rev. D55, 1280 (1997).

- [12] E. Barberis, “Higgs and SUGRA searches at the Tevatron”, Workshop on Higgs and Supersymmetry, Univ. of Florida, Gainesville, FL March 9, 1999.
- [13] T. Kamon et al., Phys. Rev. D50, 5676 (1994).
- [14] J. Gunion and T. Han, Phys. Rev. D51, 1051 (1995).

Table 1. Signal and background for Higgs signatures at Tripler.

| Signature | Signal (Background) in $20 fb^{-1}$ Higgs mass (GeV/c^2) | | | |
|----------------------|---|---------|----------|----------|
| | 150 | 200 | 300 | 500 |
| $l^\pm l^\pm l^\pm$ | 5(26) | 2(6) | 1(2) | 0.3(0.3) |
| $l^\pm l^\pm \nu\nu$ | 274(31K) | 116(8K) | 55(2.4K) | 18(400) |
| $l^\pm l^\pm jj$ | 86(1.3K) | 36(315) | 17(100) | 5.6(160) |
| χ^2 | 9 | 7 | 5 | 3 |

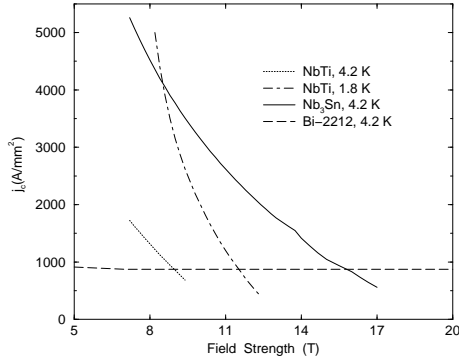


FIG. 1. Field dependence of critical current density.

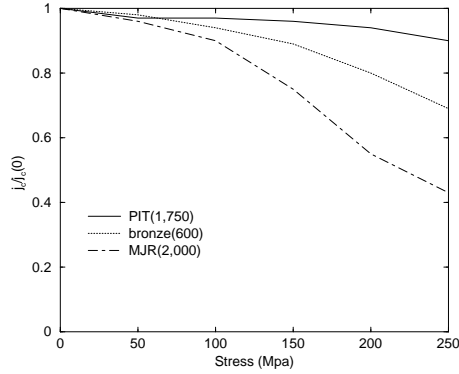


FIG. 2. Strain degradation of Nb_3Sn superconductors.

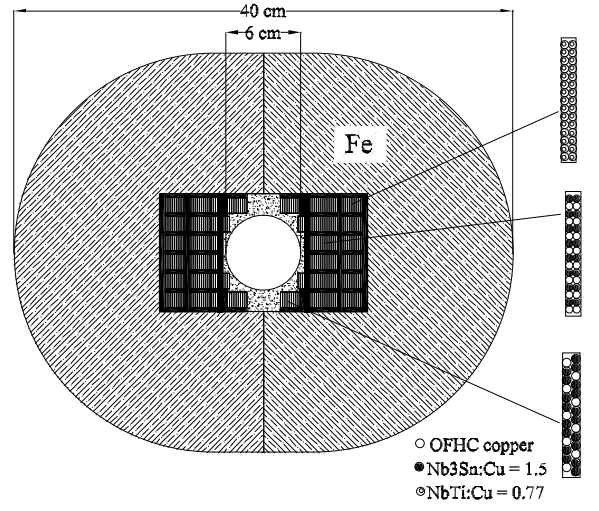


FIG. 3. Tesla dipole suitable for use in a Tevatron Tripler. Cross sections of the Rutherford coil in each section are shown.

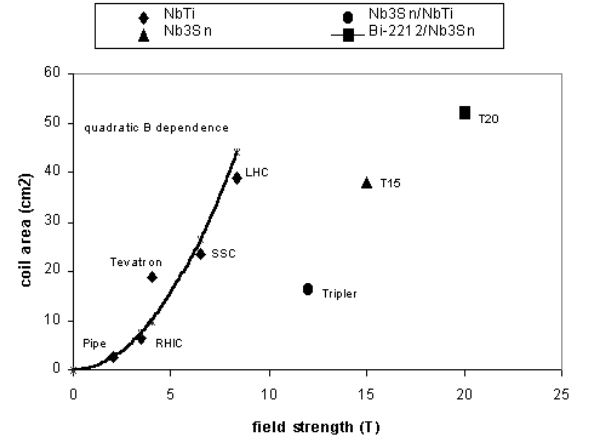


FIG. 4. Coil area for conventional dipoles and for designs using stress management and superconductor optimization.

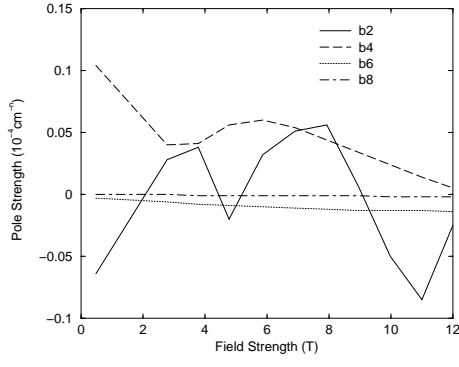


FIG. 5. Multipole moments after current programming.

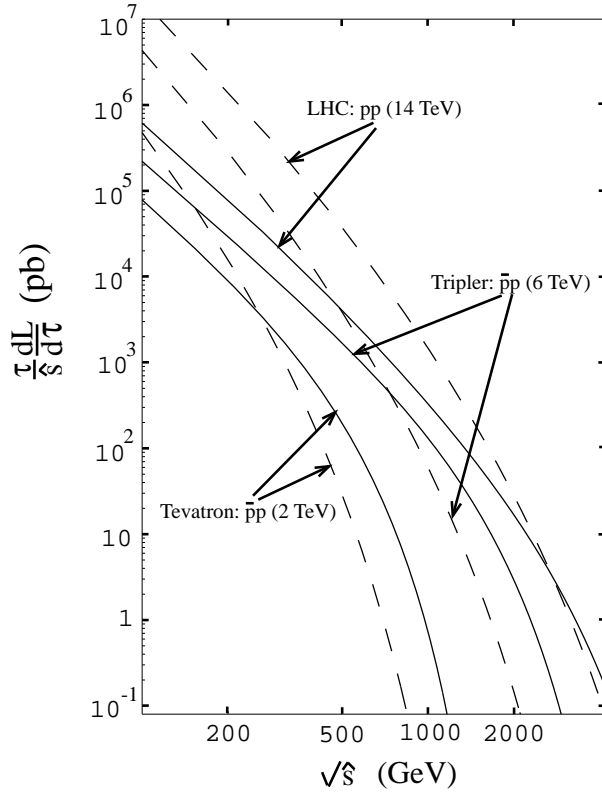


FIG. 6. Parton luminosities for $u\bar{d}$ (solid lines) and gg scattering (dashed lines).